Cell Reports, Volume *23*

Supplemental Information

Corticospinal Circuits from the Sensory and Motor Cortices Differentially Regulate Skilled Movements through Distinct Spinal Interneurons

Masaki Ueno, Yuka Nakamura, Jie Li, Zirong Gu, Jesse Niehaus, Mari Maezawa, Steven A. Crone, Martyn Goulding, Mark L. Baccei, and Yutaka Yoshida

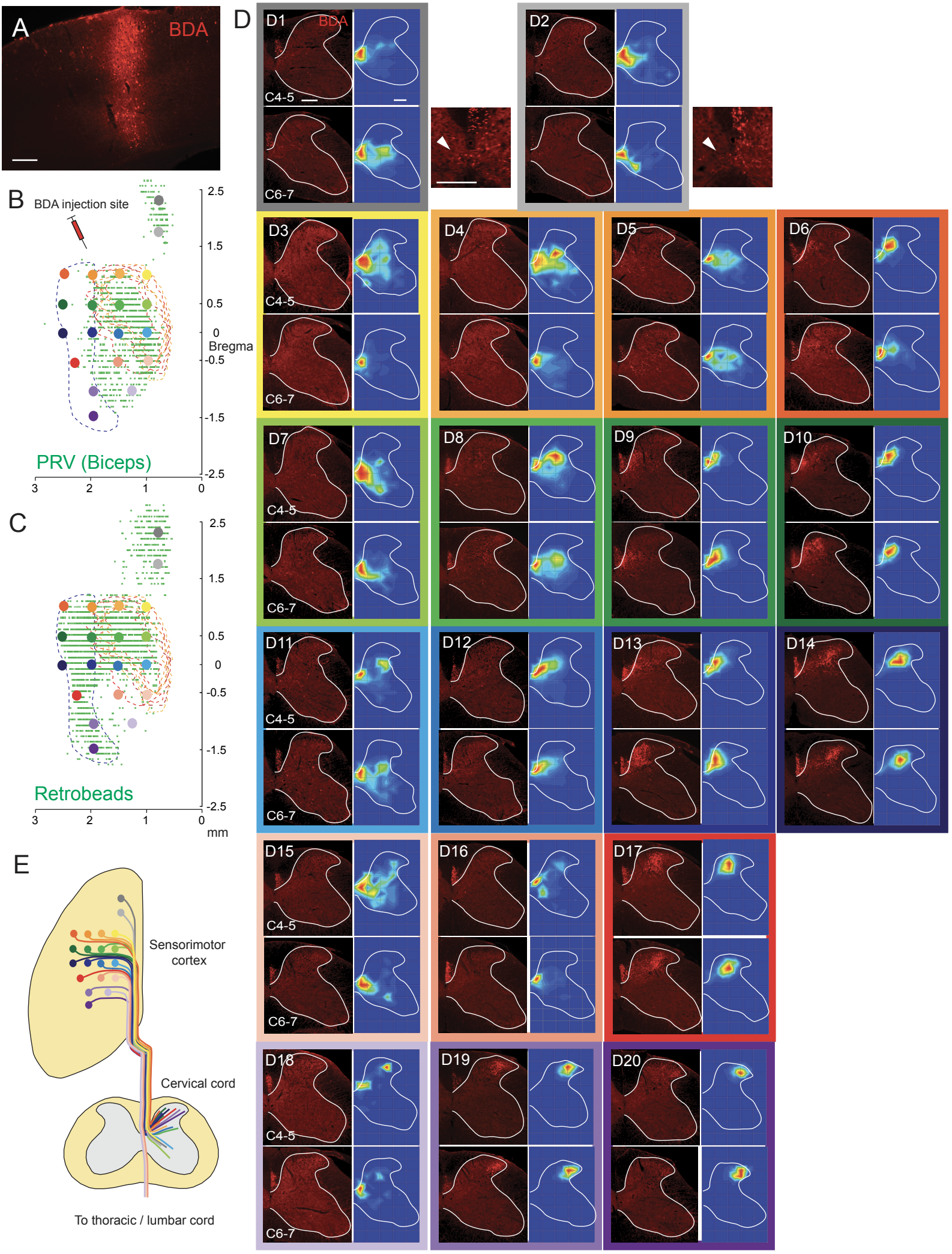
A
BDA
B
BDA injection site
PRV (Biceps)
2.5
1.5
0.5
0
Bregma
-0.5
-1.5
-2.5
3
2
1
0
C
Retrobeads
mm
D
D1
BDA
C4-5
C6-7
D2
D3
D4
D5
D6
D7
D8
D9
D10
D11
D12
D13
D14
D15
D16
D17
D18
D19
D20
E
Sensorimotor cortex
Cervical cord
To thoracic / lumbar cord

Figure S1. Projection patterns of CSTs traced from different areas of the cerebral cortex, Related to Figure 2. (A) Focal injection of BDA was restricted to the injection site in an approximately 250 μm-wide region. Coronal section of the cortex; BDA, red. Scale bar, 200 μm. (B, C) Injection sites are represented as gradual color circles (gray, yellow, red, green, blue, and purple) on the cortical map of PRV^+ (B) and $retrobeads^+$ (C) CS neurons. The blue dotted areas represent the location of lateral PRV^- / $retrobeads^+$ population, whereas the reddish orange dotted areas show the medial PRV^+ / $retrobeads^+$ population (Figure 1G). (D) Images of BDA-labeled CS fibers in spinal cord levels C4–5 and C6–7, traced from different areas as shown in (B and C). Right-hand panels show heatmaps of the distribution of CS fibers. The BDA injection site for each image is represented by the colors of the surrounding squares, which correspond to the colors of circles in (B, C). Coordinates of injection for each image are: (D1) AP 2.25 mm, ML 0.75 mm, (D2) AP 1.75 mm, ML 0.75 mm, (D3) AP 1.0 mm, ML 1.0 mm, (D4) AP 1.0 mm, ML 1.5 mm, (D5) AP 1.0 mm, ML 2.0 mm, (D6) AP 1.0 mm, ML 2.5 mm, (D7) AP 0.5 mm, ML 1.0 mm, (D8) AP 0.5 mm, ML 1.5 mm, (D9) AP 0.5 mm, ML 2.0 mm, (D10) AP 0.5 mm, ML 2.5 mm, (D11) AP 0.0 mm, ML 1.0 mm, (D12) AP 0.0 mm, ML 1.5 mm, (D13) AP 0.0 mm, ML 2.0 mm, (d14) AP 0.0 mm, ML 2.5 mm, (D15) AP -0.5 mm, ML 1.0 mm, (D16) AP -0.5 mm, ML 1.5 mm, (D17) AP -0.5 mm, ML 2.25 mm, (D18) AP -1.0 mm, ML1.25 mm, (D19) AP -1.0 mm, ML 2.0 mm, (D20) AP -1.5 mm, ML 2.0 mm. The right panels of (D1) and (D2) represent higher magnifications of midline crossing CS fibers (arrowheads). Scale bars, 200 μm. (E) Schematic diagram of the topographical projections of CS axons, illustrated by colors corresponding to (B–D). The cerebral cortex is shown from the top view, and the cervical cord is shown as a transverse image.

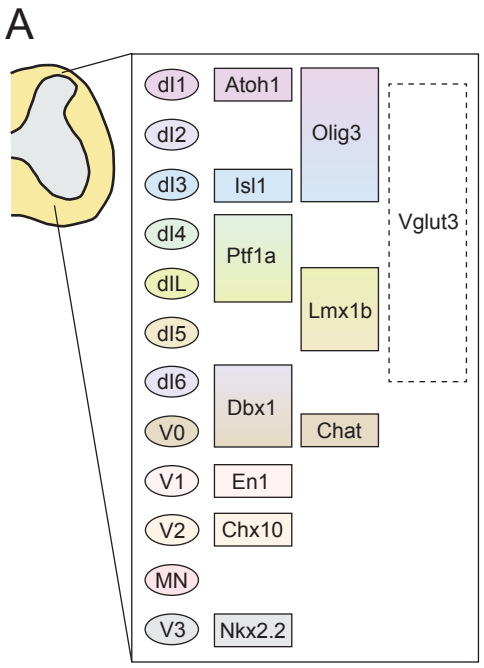

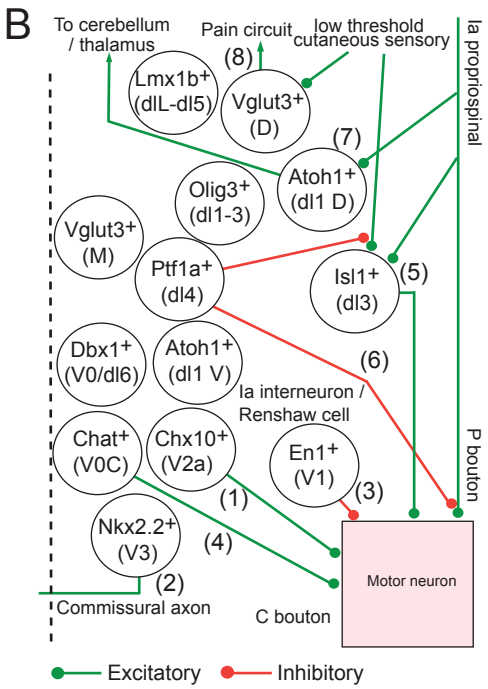

C

Genes	Subtype	Mice
Atoh1	dI1	*Math1-Cre*
Olig3	dI1–3	*Olig3-Cre*
Isl1	dI3	*Isl1-Cre*
Ptf1a	dI4–dILA	*Ptf1a-Cre*
Lmx1b	dILB–dI5	*Lmx1b-Cre*
Dbx1	dI6–V0	*Dbx1-Cre*
Chat	V0C	*Chat-Cre*
En1	V1	*En1-Cre*
Chx10	V2a	*Chx10-Cre*
Nkx2.2	V3	*Nkx2.2-Cre*
Vglut3	dorsal neurons	*Vglut3-Cre*

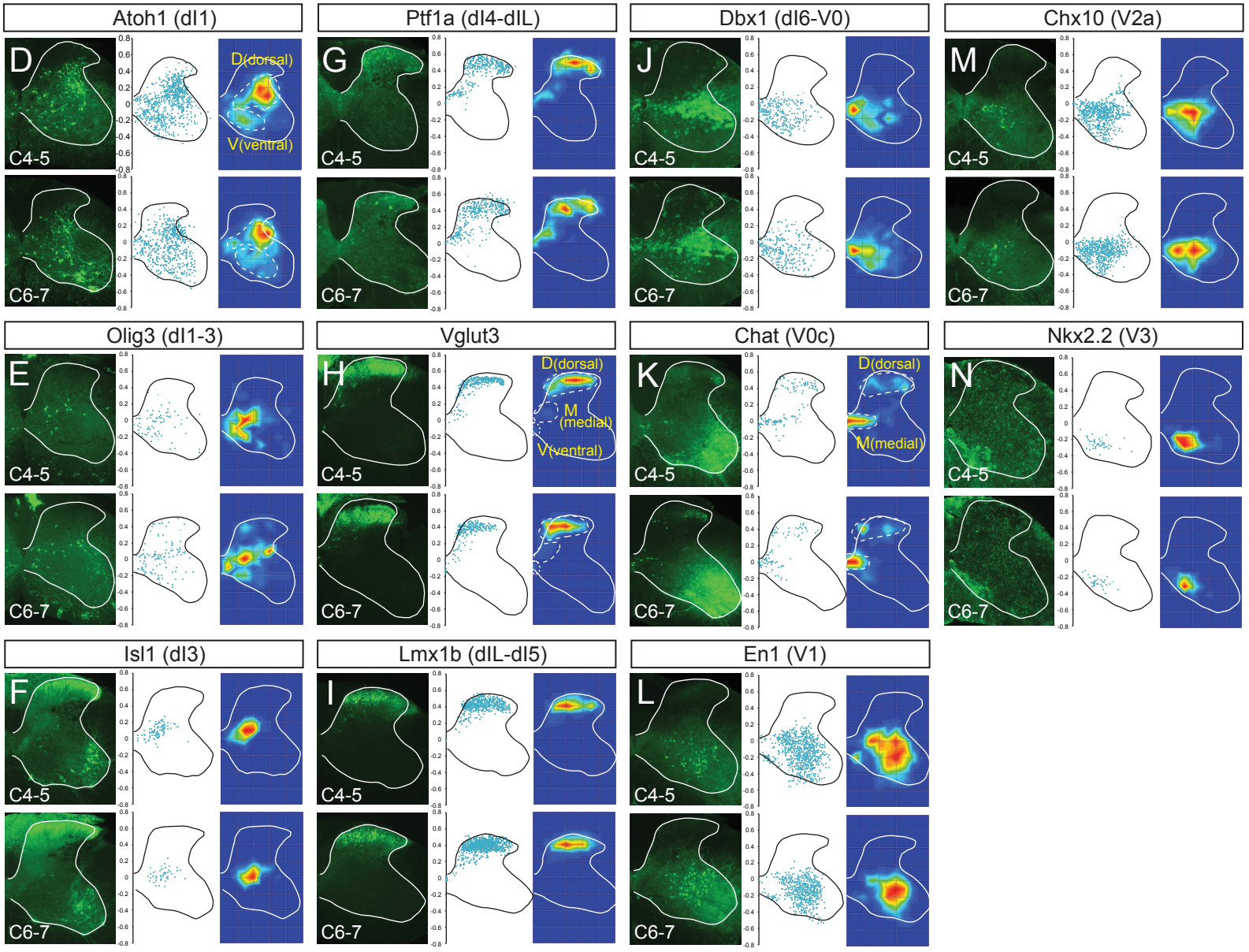

Figure S2. Subtypes of spinal IN analyzed in this study, Related to Figure 3. (A) The diagram of spinal IN subtypes (dI1–V3) in the spinal cord (Alaynick et al., 2011). The marker genes to identify the IN subtypes in this study are shown in the right side. (B) The original connectivity map of spinal INs, based on previous reports (related to Figure 3K–3L): (1) (Azim et al., 2014), (2) (Zhang et al., 2008), (3) (Alvarez et al., 2005; Sapir et al., 2004), (4) (Stepien et al., 2010; Zagoraiou et al., 2009), (5) (Bui et al., 2013), (6) (Betley et al., 2009), (7) (Bermingham et al., 2001; Yuengert et al., 2015), (8) (Peirs et al., 2015). Green lines represent excitatory connections; red lines represent inhibitory connections. For clarity, not all connections of INs are shown. (C) The list of interneuron populations analyzed in this study: Atoh1^{+} (Math1-Cre for dI1 (Bermingham et al., 2001; Lee et al., 1998)), Olig3^{+} (Olig3-Cre for dI1–3 (Muller et al., 2005)), Isl1^{+} (Isl1-Cre for dI3 (Bui et al., 2013; Gross et al., 2002; Muller et al., 2002)), Ptf1a^{+} (Ptf1a-Cre for dI4–dILA (Betley et al., 2009)), Lmx1b^{+} (Lmx1b-Cre for dILB–dI5 (Gross et al., 2002; Muller et al., 2002)), Dbx1^{+} (Dbx1-Cre for dI6–V0 (Pierani et al., 2001)), Chat^{+} (Chat-Cre for V0C (Zagoraiou et al., 2009)), En1^{+} (En1-Cre for V1 (Sapir et al., 2004)), Chx10^{+} (Chx10-Cre for V2a (Azim et al., 2014; Crone et al., 2008)), Nkx2.2^{+} (Nkx2.2-Cre for V3 (Briscoe et al., 1999)), and Vglut3^{+} INs (Vglut3-Cre for dorsal INs (Peirs et al., 2015)). (D–N) Distribution of spinal INs in the cervical cord. Spinal IN subtypes were labeled by *Atoh1-Cre*; *CC-EGFP* (D), *Olig3-Cre*; *CC-EGFP* (E), *Isl1-Cre*; *CC-EGFP* (F), *Ptf1a-Cre*; *CC-EGFP* (G), *Vglut3-Cre*; *CC-EGFP* (H), *Lmx1b-Cre*; *CC-EGFP* (I), *Dbx1-Cre*; *CC-EGFP* (J), *Chat-Cre*; *CC-EGFP* (K), *En1-Cre*; *CC-EGFP* (L), *Chx10-Cre*; *CC-EGFP* (M), and *Nkx2.2-Cre*; *CC-EGFP* mice (N). Panels on the left shows representative images of GFP^{+} spinal INs in the transverse spinal cord at levels C4–5 and C6–7, middle panels show plots of GFP^{+} neurons, and panels on the right show heatmaps of the distributions of the GFP^{+} neurons. The X, Y origin (0, 0) corresponds to the position of the central canal. The lines indicate one representative margin of the gray matter. As indicated by the dotted lines in the heatmaps, *Atoh1*-GFP^{+}, *Vglut3*-GFP^{+}, and *Chat*-GFP^{+} INs were subdivided as D (dorsal) / V (ventral), D / M (medial) / V, and D / M population, respectively. Scale bars, 200 μm.

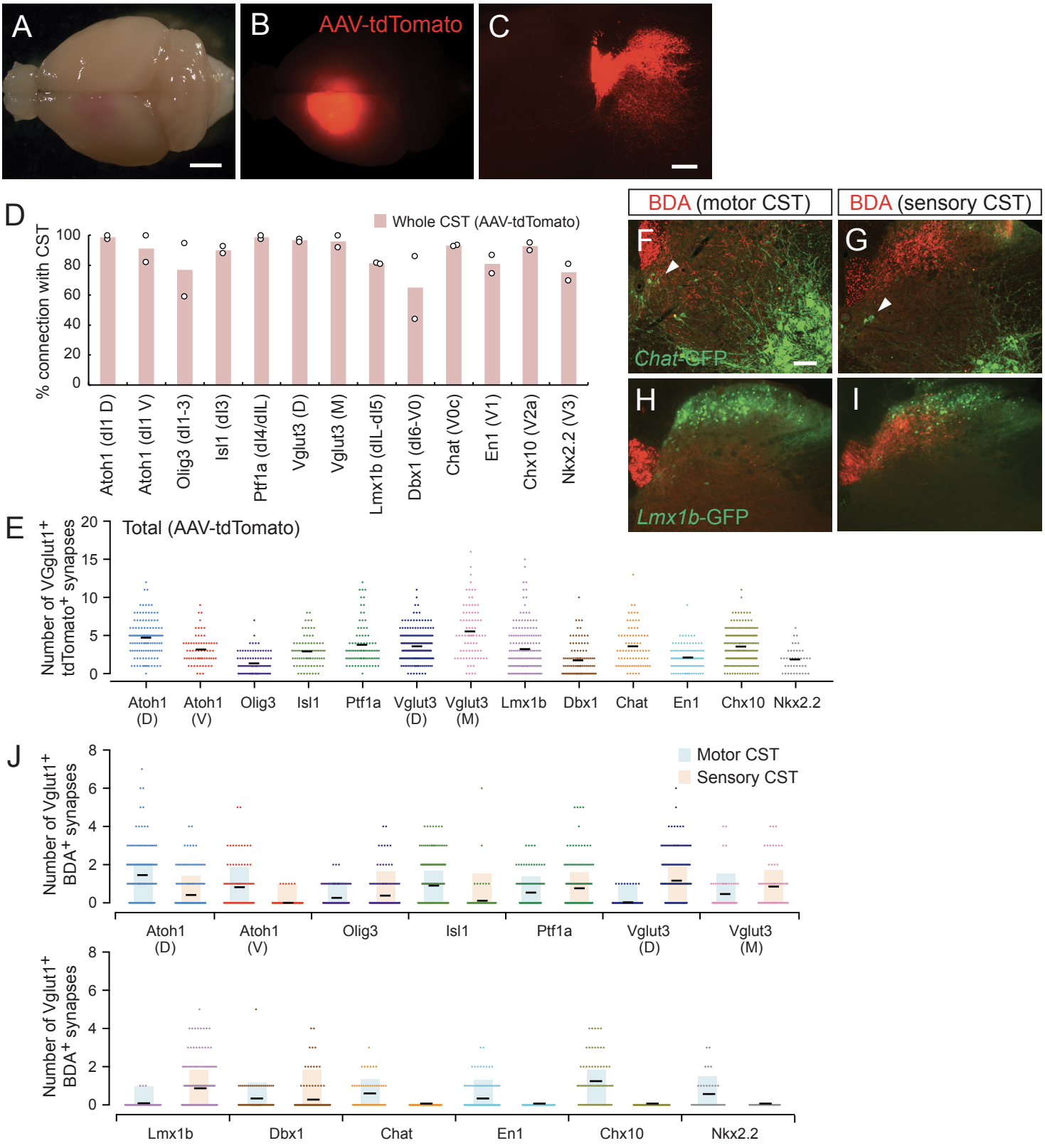

Figure S3. Connectivity between CS axons and spinal INs, Related to Figure 3. (A–C) Injections of high titer AAV1-CAG-tdTomato labeled broad cortical areas with CS fibers. Gross appearance of the brain and tdTomato$^+$ fluorescent expression (A, B), and tdTomato$^+$ CS fibers in a transverse section of the cervical cord. Scale bars, 2 mm (A), 200 μm (C). (D) Ratio of spinal INs connected with the entier CST labeled with AAV1-CAG-tdTomato. Bars indicate average ratios with a value for each animal indicated by a white circle (n = 2 animals). (E) Numbers of Vglut1$^+$ presynaptic terminals of AAV-tdTomato-labeled CS axons on GFP$^+$ spinal INs. Lines indicate the mean numbers of synapses of the neurons examined. (F–I) Representative images of motor (F, H) and sensory CS axons (G, I) labeled with BDA (red), and Chat-GFP$^+$ and Lmx1b-GFP$^+$ spinal INs in *Chat-Cre*; *CC-EGFP* (F, G); *Lmx1b-Cre*; *CC-EGFP* (H, I) mice. Scale bar, 100 μm. (J) Number of Vglut1$^+$ presynaptic terminals of BDA-labeled motor and sensory CS axons on GFP$^+$ spinal INs. Bars indicate the mean numbers of synapses of neurons having connection with motor (light blue) and sensory CS axons (light orange). These values were used for calculations in Figures 3K and 3L. Lines indicate the mean numbers of synapses of all the neurons examined (including non-connecting INs).

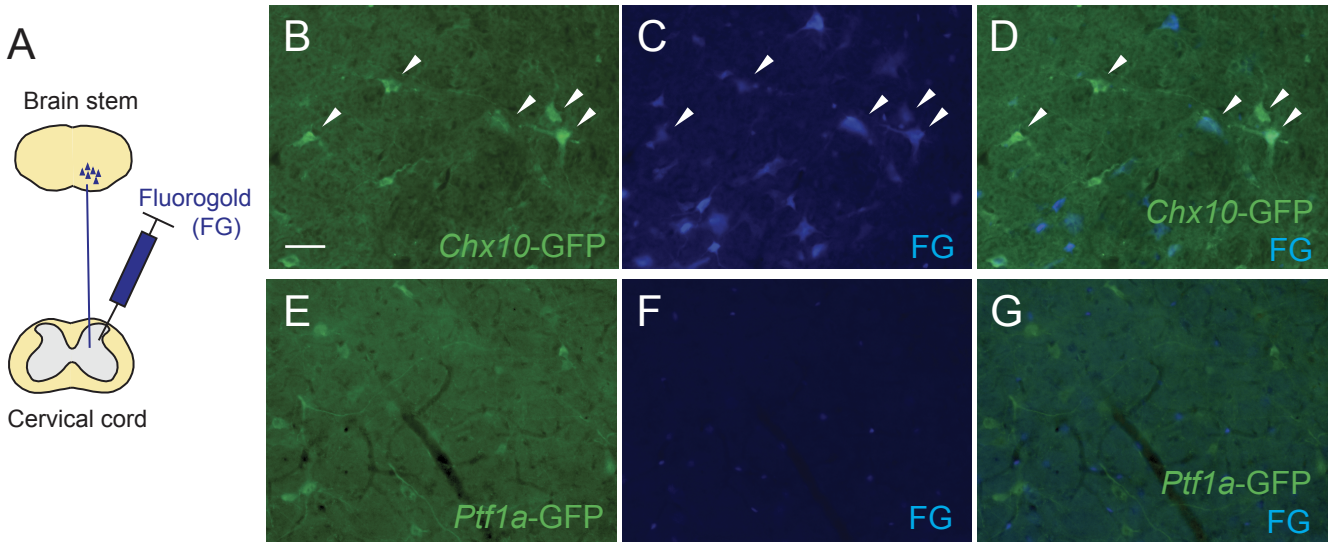

Figure S4. Retrograde tracing of brain stem neurons from the cervical cord, Related to Figure 4. (A) Diagram of retrograde tracing using fluorogold (FG), injected into the cervical cord. (B–D) Representative coronal section images of *Chx10*-GFP$^+$ and FG$^+$ neurons in the brain stem (reticular nucleus) of *Chx10-Cre*; *CC-EGFP* mice. Arrowheads indicate *Chx10*-GFP$^+$ / FG$^+$ neurons. (E–G) Representative coronal section images of *Ptf1a*-GFP$^+$ and FG$^+$ neurons in the dorsal region of the medulla in *Ptf1a-Cre*; *CC-EGFP* mice. No double positive neurons were observed. Scale bar, 50 μm.

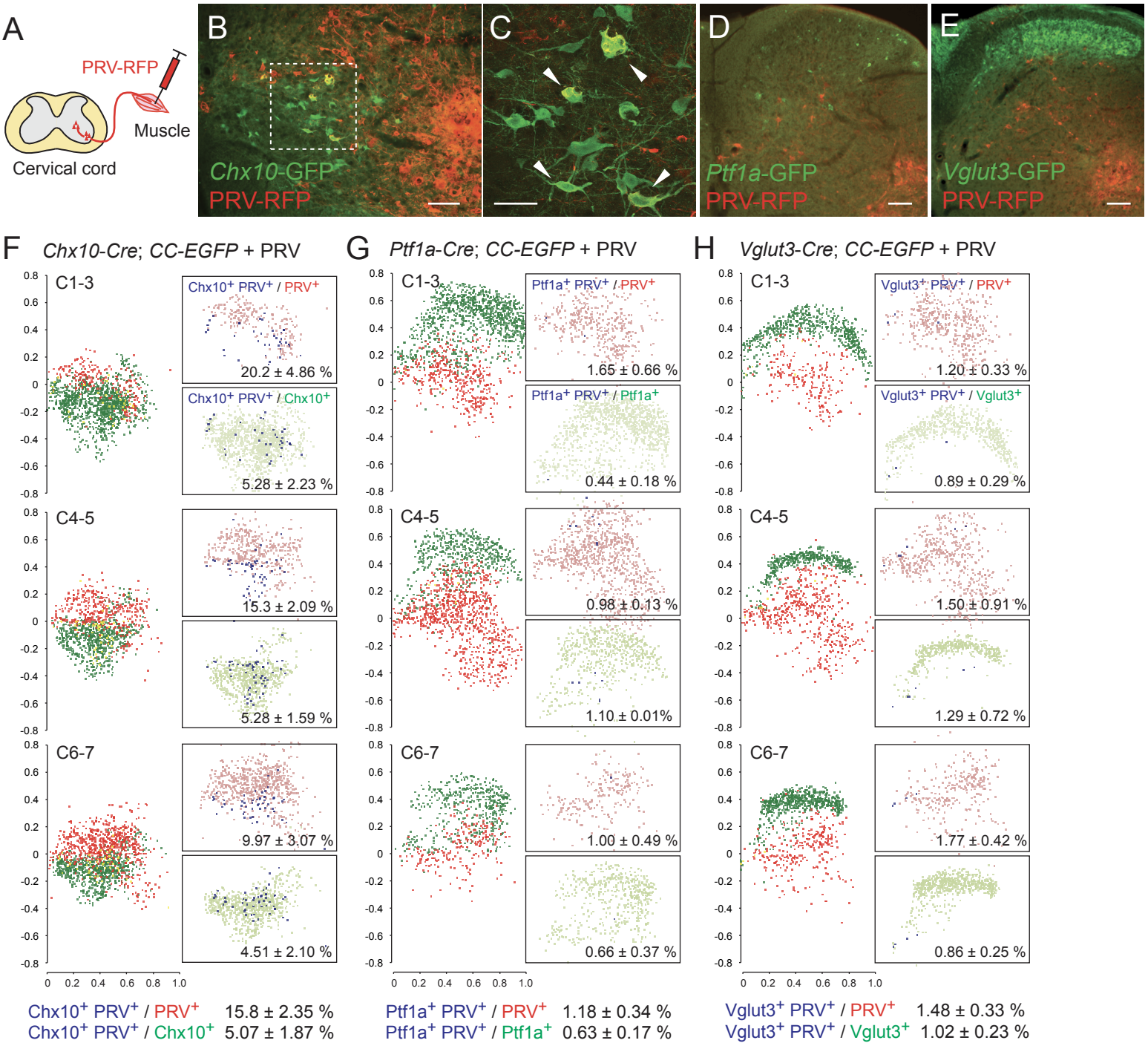

Figure S5. Retrograde trans-synaptic tracing of spinal INs from forelimb muscles, Related to Figure 6. (A) Diagram of PRV-RFP injection and tracing of spinal INs. (B–E) Representative transverse images of PRV-labeled *Chx10*-GFP$^+$ (B, C), *Ptf1a*-GFP$^+$ (D), and *Vglut3*-GFP$^+$ (E) neurons in the cervical cord at the C4 level in *Chx10-Cre*; *CC-EGFP*, *Ptf1a-Cre*; *CC-EGFP*, and *Vglut3-Cre*; *CC-EGFP* mice. PRV-RFP (red), GFP (green). (C) is a magnified view of the dotted square in (B). Arrowheads indicate PRV-RFP$^+$ / *Chx10*-GFP$^+$ neurons. Scale bars, 100 μm (B, D, E), 50 μm (C). (F–H) Localization of PRV-RFP$^+$ and *Chx10*-GFP$^+$ (E), *Ptf1a*-GFP$^+$ (F), *Vglut3*-GFP$^+$ (G) neurons in the cervical cord (each from one representative animal). Each dot corresponds to one neuron. The X, Y origin (0, 0) corresponds to the position of the central canal. Data are represented as mean ± SEM. (Chx10, n = 4; Ptf1a, n = 3; Vglut3, n = 3).

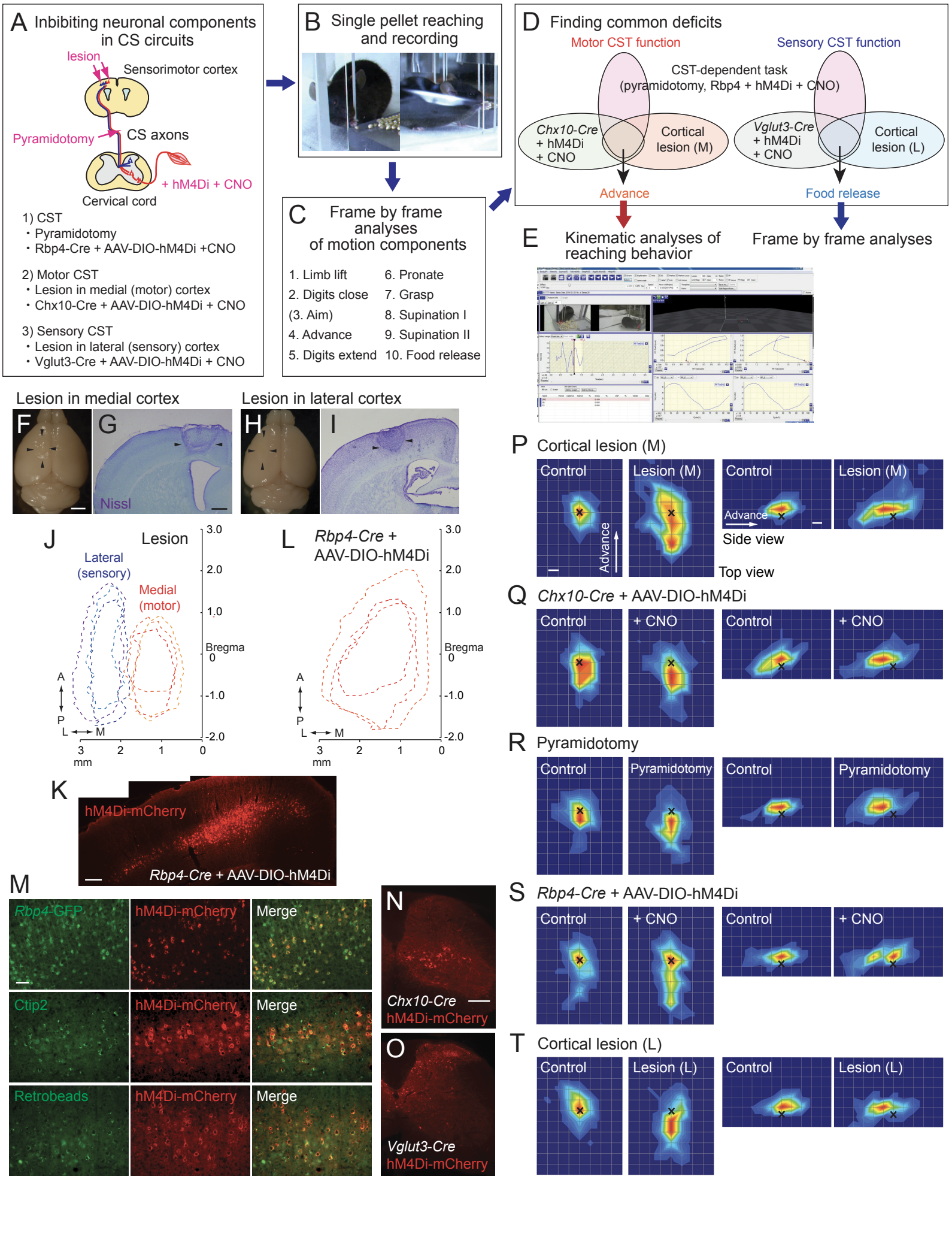
A Inbibiting neuronal components in CS circuits
lesion
Sensorimotor cortex
Pyramidotomy
CS axons
+ hM4Di + CNO
Cervical cord
1) CST
• Pyramidotomy
• Rbp4-Cre + AAV-DIO-hM4Di +CNO
2) Motor CST
• Lesion in medial (motor) cortex
• Chx10-Cre + AAV-DIO-hM4Di + CNO
3) Sensory CST
• Lesion in lateral (sensory) cortex
• Vglut3-Cre + AAV-DIO-hM4Di + CNO
B Single pellet reaching and recording
C Frame by frame analyses of motion components
1. Limb lift
2. Digits close
(3. Aim)
4. Advance
5. Digits extend
6. Pronate
7. Grasp
8. Supination I
9. Supination II
10. Food release
D Finding common deficits
Motor CST function
Sensory CST function
CST-dependent task
(pyramidotomy, Rbp4 + hM4Di + CNO)
Chx10-Cre + hM4Di + CNO
Cortical lesion (M)
Vglut3-Cre + hM4Di + CNO
Cortical lesion (L)
Advance
Food release
E Kinematic analyses of reaching behavior
Frame by frame analyses
Lesion in medial cortex
Lesion in lateral cortex
F
G
Nissl
H
I
J Lesion
Lateral (sensory)
Medial (motor)
Bregma
3.0
2.0
1.0
0
-1.0
-2.0
A
P
L
M
3
2
1
0
mm
L Rbp4-Cre + AAV-DIO-hM4Di
K
hM4Di-mCherry
Rbp4-Cre + AAV-DIO-hM4Di
M
Rbp4-GFP
hM4Di-mCherry
Merge
Ctip2
Retrobeads
N
Chx10-Cre
hM4Di-mCherry
O
Vglut3-Cre
hM4Di-mCherry
P Cortical lesion (M)
Control
Lesion (M)
Advance
Side view
Top view
Q Chx10-Cre + AAV-DIO-hM4Di
+ CNO
R Pyramidotomy
Pyramidotomy
S Rbp4-Cre + AAV-DIO-hM4Di
T Cortical lesion (L)
Lesion (L)

Figure S6. Analyses of skilled motor behaviors in mice subjected to silencing or ablating neurons in motor and sensory CS circuits, Related to Figure 7. (A–E) Experimental work flow to investigate functions of motor and sensory CS circuits during skilled behaviors**.** (A) Diagram showing the neuron silencing and ablating experiments involved in motor and sensory CS circuits. Approaches to 1) inhibit global CS circuitry (pyramidotomy and layer V inhibition by *Rbp4-Cre* mice + AAV-DIO-hM4Di + CNO), 2) to inhibit motor CS circuits (medial (motor) cortex lesioning and *Chx10-Cre* mice + AAV-DIO-hM4Di + CNO), and 3) to inhibit sensory CS circuit (lesion in the lateral (sensory) cortex and *Vglut3-Cre* mice + AAV-DIO-hM4Di + CNO) are illustrated. (B) Mice were subjected to the single pellet reaching task and the behaviors were recorded by high-speed cameras. (C) Motion components were scored by frame by frame analyses, according to the criteria reported previously (Whishaw, 1996)(related to Figure 7H–7O). (D) Common deficits exhibited by motor or sensory CST-related inhibition were found to reveal motor or sensory CST functions in skilled behaviors. (E) Detailed kinematic or frame by frame analyses were conducted on motion components found in (D) (related to Figures 7P–7W). (F–O) Lesions and introduced hM4Di expression in the motor and sensory CS circuits. (F–I) Representative images of focal stroke lesions in the medial (motor) (F, G) and lateral (sensory) cortex (H, I). Coronal sections with Nissl staining (G, I). Arrowheads indicate lesioned areas. Scale bars, 2 mm (F, H), 200 μm (G, I). (J) Areas of focal lesions in the medial (red) and lateral cortex (blue) of 3 representative animals. Top view of the cortex. (K) Representative coronal section images of hM4Di-mCherry expression (red) in the cerebral cortex of a layer V-specific *Rbp4-Cre*; *CC-EGFP* mouse injected with AAV-DIO-hM4Di-mcherry. Scale bar, 200 μm. (L) hM4Di-mCherry$^+$ areas in the cerebral cortex of *Rbp4-Cre* mice (3 representative animals). Top view of the cortex. (M) Representative coronal section images of hM4Di-mCherry expression (red) in layer V of a *Rbp4-Cre* mouse injected with AAV-DIO-hM4Di-mcherry. Top panels: hM4Di-mCherry and EGFP expression (green) in *Rbp4-Cre*; *CC-EGFP* mouse. Middle panels: hM4Di-mCherry and Ctip2 expression (green, a layer V marker). Bottom panels: hM4Di-mCherry expression and CS neurons retrogradely labeled with retrobeads (green). Scale bar, 100 μm. (N, O) Representative images of hM4Di-mCherry expression in the cervical cords of *Chx10-Cre* + AAV-DIO-hM4Di-mcherry (N), and *Vglut3-Cre* + AAV-DIO-hM4Di-mcherry mice (O). Transverse sections, hM4Di-mCherry (red). Scale bar, 200 μm. (P–T) Kinematic analyses of aberrant reaching in the advancement phase in mice with medial (motor) cortex lesions (P), silencing Chx10$^+$ neurons (Q), with pyramidotomies (R), silencing Rbp4$^+$ layer V neurons (S), and with lateral (sensory) cortex lesions (T). Related to Figures 7P–T. The heatmaps show the spatial probabilities of the far distal positions of the reaching paw relative to the position of the pellet ("x"). The two left panels show top views, where the direction of forelimb advancement is from bottom to top (same figures with Figures 7P–T). The two right panels show side views, with the forelimb advancing from left to right. Data is shown for 1) mice with lesions in the medial cortex (control, 78 reaches; injury, 121 reaches), 2) *Chx10-Cre* mice + AAV-DIO-hM4Di (control, 84 reaches; post-CNO injection, 109 reaches), 3) mice with pyramidotomies (control, 88 reaches; injury, 118 reaches), 4) *Rbp4-Cre* mice + AAV-DIO-hM4Di (control, 64 reaches; post-CNO injection, 110 reaches), and 5) mice with lesions in the lateral cortex (control, 64 reaches; injury, 92 reaches). Scale bars (1 division), 2 mm.

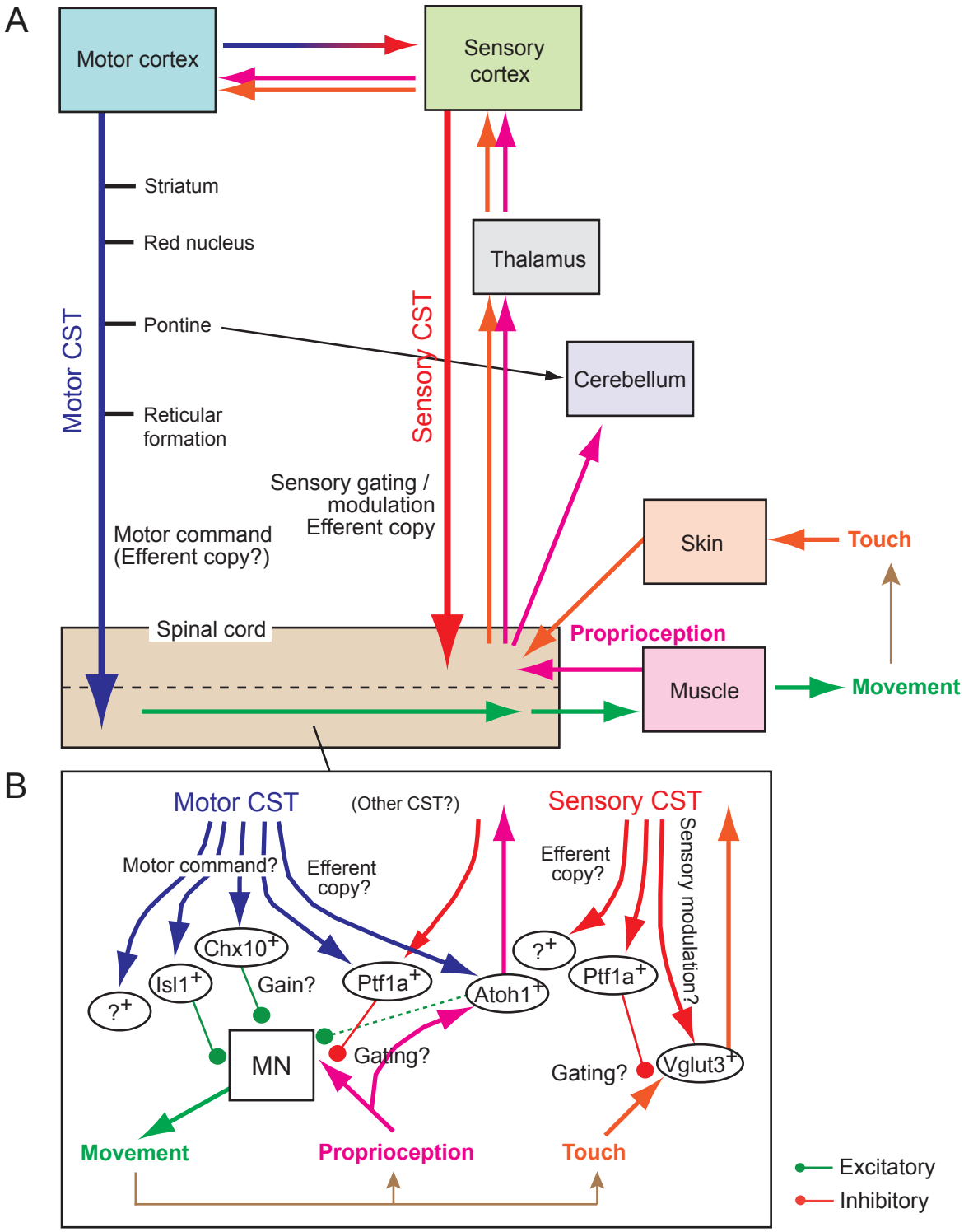

Figure S7. Schematic diagram of connectivity and functions of motor and sensory CS circuit (proposed model), Related to Figure 7. (A) The CS system is composed of at least 2 parallel projections from the motor and sensory cortex to the spinal cord. The motor CS fibers project to the intermediate/ventral part of the spinal cord and engage in execution of motor command which signals through premotor INs-motor neurons (MN)-muscles (blue to green arrows). This circuit may also contain efferent copy information (Hantman and Jessell, 2010). Sensory CS circuit sends top down signals to the dorsal spinal cord (a red arrow), to gate cutaneous and proprioceptive sensory information that input into the spinal cord (orange and pink arrows), and/or send efferent copies of movements which might contain tactile and proprioceptive sensory information during motor tasks. The top-down signals from the sensory cortex to the spinal cord might be generated by the signals from the motor cortex (a blue-red gradient arrow) (Manita et al., 2015). (B) Distinct connections of motor and sensory CSTs in the spinal cord. Motor CSTs (blue arrows) connect abundantly with premotor neurons, which would be the neural substrates for motor execution. Although we found Chx10^{+} neurons as the target of motor CSTs to gain the speed of movement, other spinal INs might be involved in other parameters for motor execution. Sensory CS fibers (red arrows) connect with sensory-related excitatory and inhibitory neurons, which control the gain of sensory information ("gating" or sensory modulation) or mediate the signals of efferent copies. These top-down sensory signals might be required to smooth out the execution of complex sequential behaviors which receives continuous cutaneous and proprioceptive sensory information (brown arrows). Our anterograde tracing experiments also implicate a presence of other types of CS system. See the details in Discussion.